Science Advances
AAAS

Supplementary Materials for

Therapeutic blockade of ER stress and inflammation prevents NASH and progression to HCC

Ebru Boslem *et al.*

Corresponding author: Mark A. Febbraio, mark.febbraio@monash.edu

Sci. Adv. **9**, eadh0831 (2023)
DOI: 10.1126/sciadv.adh0831

The PDF file includes:

Figs. S1 to S14
Legends for tables S1 to S6

Other Supplementary Material for this manuscript includes the following:

Tables S1 to S6

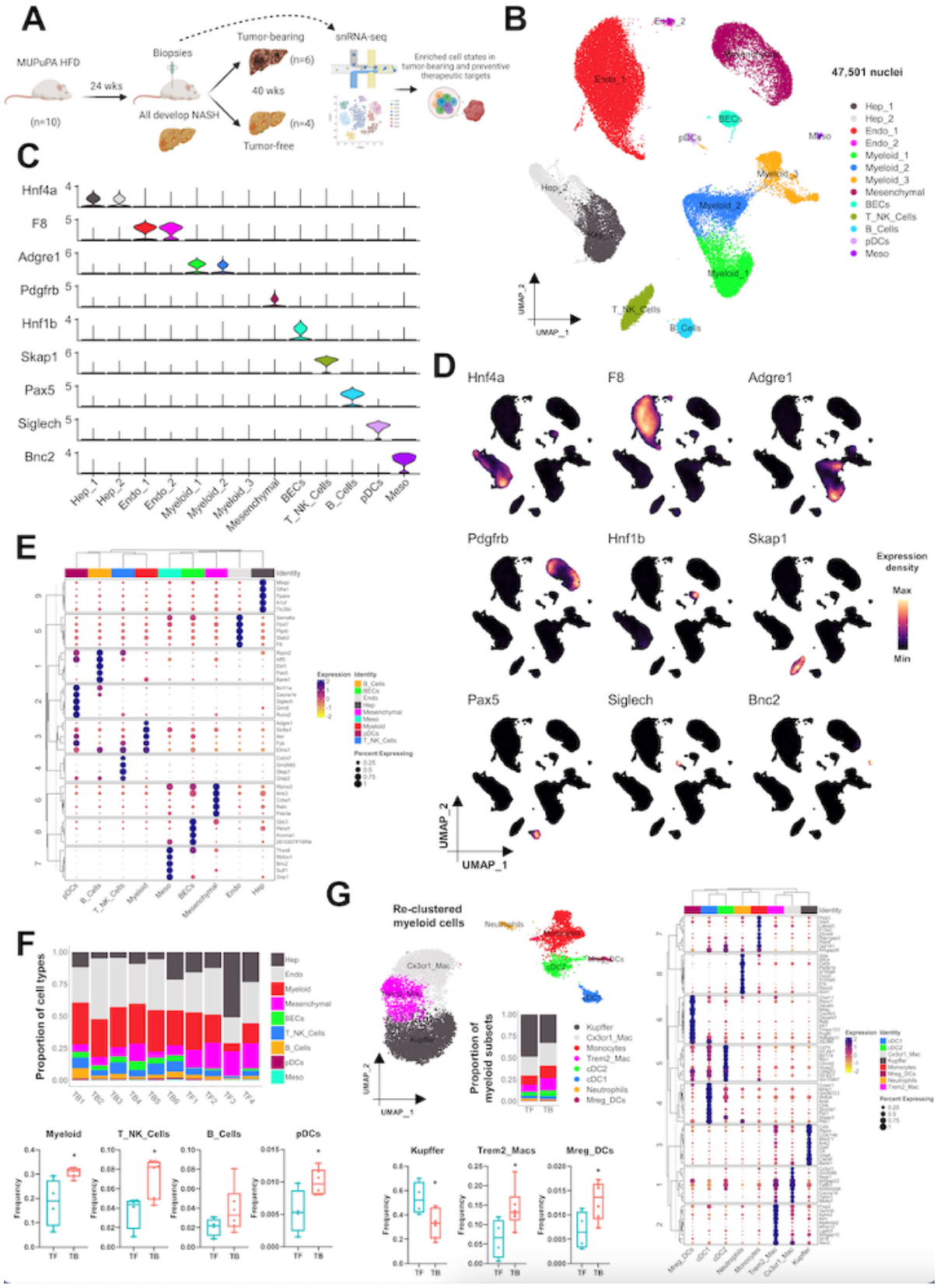
A
MUPuPA HFD
(n=10)
24 wks
Biopsies
All develop NASH
Tumor-bearing
(n=6)
40 wks
(n=4)
Tumor-free
snRNA-seq
Enriched cell states in tumor-bearing and preventive therapeutic targets
B
47,501 nuclei
Hep_1
Hep_2
Endo_1
Endo_2
Myeloid_1
Myeloid_2
Myeloid_3
Mesenchymal
BECs
T_NK_Cells
B_Cells
pDCs
Meso
C
Hnf4a
F8
Adgre1
Pdgfrb
Hnf1b
Skap1
Pax5
Siglech
Bnc2
D
Expression density
Max
Min
UMAP_1
UMAP_2
E
Identity
Expression
Percent Expressing
F
Proportion of cell types
TB1
TB2
TB3
TB4
TB5
TB6
TF1
TF2
TF3
TF4
Myeloid
T_NK_Cells
B_Cells
pDCs
Frequency
TF
TB
G
Re-clustered myeloid cells
Neutrophils
Mreg_DCs
cDC1
cDC2
Cx3cr1_Mac
Kupffer
Monocytes
Trem2_Mac
Proportion of myeloid subsets
Kupffer
Trem2_Macs
Mreg_DCs

Supplementary Figure 1. Experimental design and single nucleus RNA sequencing (snRNA-seq) clustering and annotation.(A) Experimental design and workflow to discovery of enriched cell states in NASH to HCC conversion. (B) UMAP visualization and cell type annotation of clustered 47,501 single nuclei from n=10 liver biopsies of high fat diet (HFD) fed MUPuPA mice at 24 weeks post experimental start. Hepatocytes (Hep_1 and Hep_2), endothelial cells (Endo_1 and Endo_2), myeloid (Myeloid_1, Myeloid_2 and Myeloid_3), mesenchymal, biliary epithelial cells (BECs), T and natural killer cells (T_NK_Cells), B cells, plasmacytoid dendritic cells (pDCs) and mesothelial cells (Meso). (C) Violin plot showing expression of cell type specific marker genes. Hnf4a (Hep), F8 (Endo), Adgre1 (myeloid), Pdgfrb (mesenchymal), Hnf1b (BECs), Skap1 (T_NK_Cells), Pax5 (B_Cells), Siglech (pDCs) and Bnc2 (Meso). (D) Expression of cell type specific marker genes in the UMAP space. (E) Dot plot generated using scCustomize showing expression levels and detection percentages of top 5 genes in each cell type, organized based on hierarchical clustering results of both gene expression patterns and cell type identities. (F) (Top) relative frequencies of hepatic cell types in each sample. (Bottom) box and whisker plots showing frequencies of immune cell types according to HCC outcome. *$p < 0.05$ by unpaired t test, TF, n=4 and TB, n=6. (G) (Top left) UMAP visualization of re-clustered myeloid cells with eight subsets identified as indicated. Relative frequencies of each subset are displayed for combined TF and TB samples. (Bottom left) box and whisker plots showing frequencies of myeloid subsets that displayed statistically significant differential enrichment in TB vs TF. *$p < 0.05$ by unpaired t test, TF, n=4 and TB, n=6. (Right) Dot plot showing expression levels and detection percentages of top 10 genes in each myeloid subset, organized based on hierarchical clustering results of both gene expression patterns and subset identities.

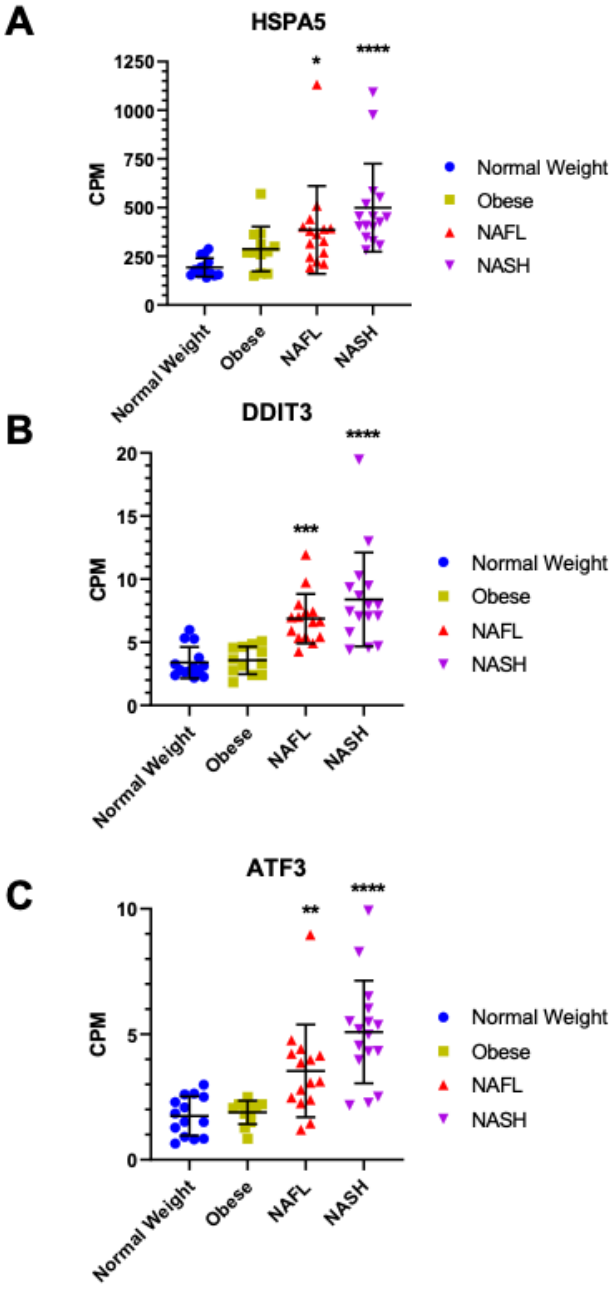

Supplementary Figure 2. Expression levels of ER Stress related genes in humans with fatty liver disease. (A) Heat Shock Protein Family A (Hsp70) Member 5 (HSPA5), (B) DNA damage inducible transcript 3 (DDIT3), (C) Activating transcription factor 3 (ATF3) obtained from a publicly available bulk RNAseq dataset (GSE126848) where subjects were grouped according to stage in NAFLD spectrum (normal, obese, NAFL and NASH) (see reference 42). Data are expressed as mean ± SEM. **p<0.05, **p<0.01, ***p<0.001, ****p,0.0001.*

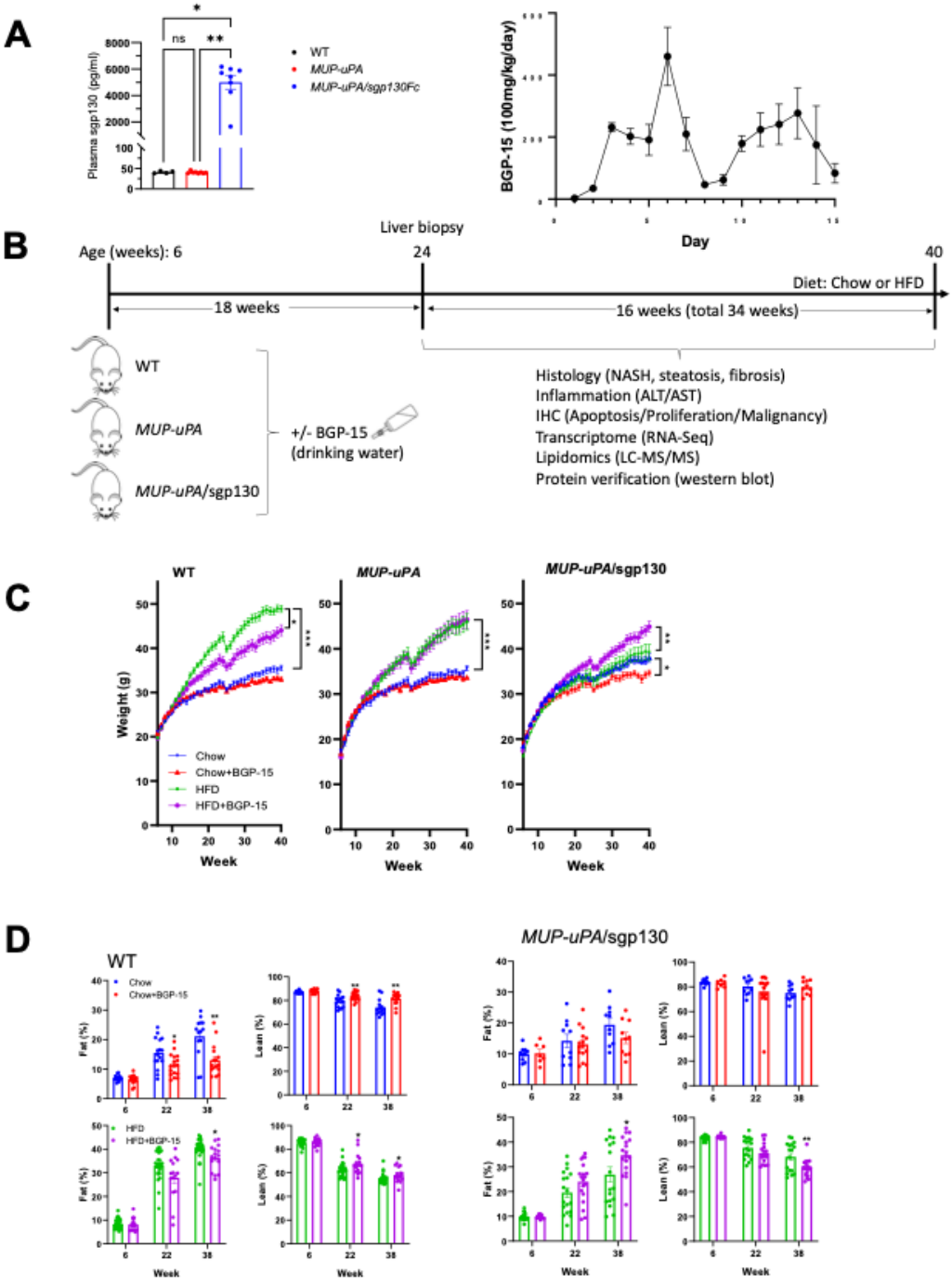

Supplementary Figure 3. Treatment of *MUP-uPA/sgp130Fc* mice with BGP-15 affects body mass and liver injury. Plasma levels of sgp130 (A), and of BGP-15 (B) in mice. Plasma sgp130 levels in mice (A). BGP-15 levels in the blood during pilot experiment (B) Experimental design (C). Body weight (C) and percent fat mass (D) over the duration of the experimental intervention in wild type (WT) mice, *MUP-uPA* mice and *MUP-uPA*/sgp130 mice fed a chow or a high fat diet (HFD) and treated with or without BGP-15. Data were analysed by one-way Freidman's (non-parametric) ANOVA with Dunn's multiple comparisons between groups indicated. The following numbers of biological replicates were used (independent mice) per group in each experiment: (A) = 6-8, (B) = 5, (C-D) =14-26. Data are expressed as mean ±SEM . *$p<0.05$, **$p<0.01$, ***$p<0.001$.

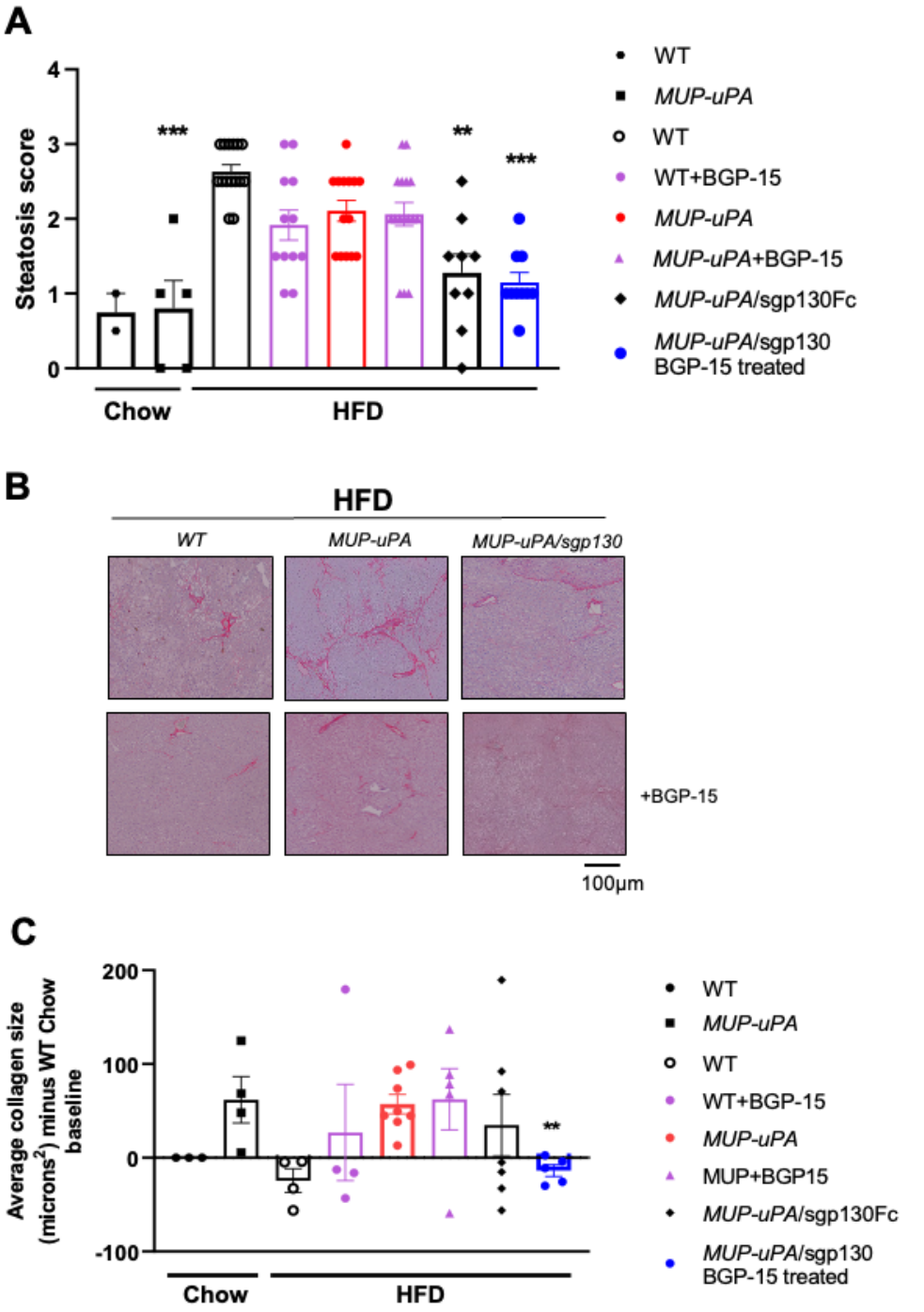

Supplementary Figure 4. Treatment of *MUP-uPA/sgp130Fc* mice with BGP-15 affects markers of NASH at 24 weeks. Steatosis measured via Hematoxylin and Eosin (H & E) staining (A) representative Picosirus Red (PSR) staining (B) and quantification (C) at 24 wk (biopsy) in wild type (WT) mice, *MUP-uPA* mice and *MUP-uPA*/sgp130 mice fed a chow or a high fat diet (HFD) and treated with or without BGP-15. Data were analysed by one-way sample t test against a theoretical mean of zero. The following numbers of biological replicates were used (independent mice) per group in each experiment: (A) = 2-16; (C) = 3-8. Data are expressed as mean ±SEM . ***p<0.01*, ****p<0.001* compared with *MUP-uPA* HFD .

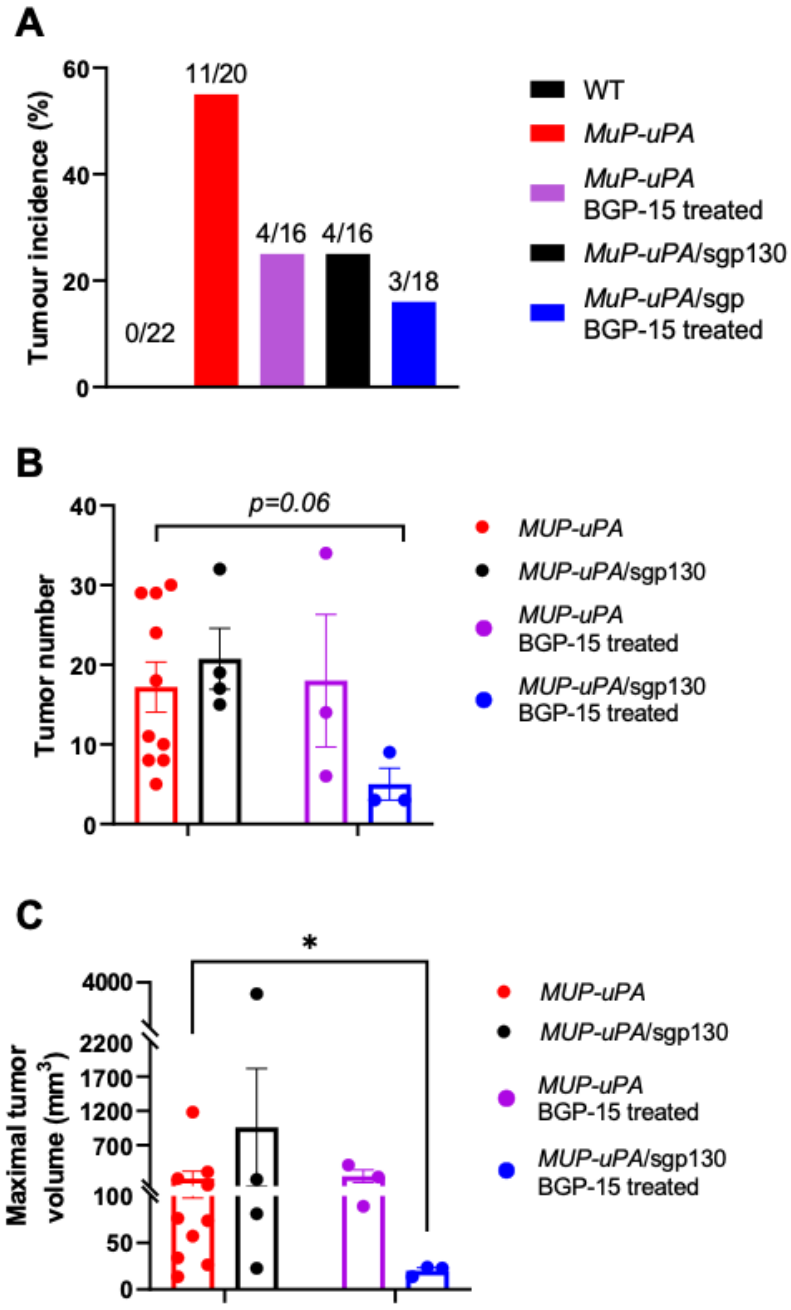

Supplementary Figure 5. Treatment of *MUP-uPA/sgp130Fc* mice with BGP-15 affects HCC at 40 weeks. Tumor incidence (A), tumor number (B) and tumor volume (C) in *MUP-uPA* mice, *MUP-uPA*/sgp130 mice, MUP-uPA mice treated with BGP-15 and *MUP-uPA*/sgp130 mice treated with BGP-15 fed high fat diet (HFD). Data were analysed by one-way sample t test against a theoretical mean of zero. The following numbers of biological replicates were used (independent mice) per group in each experiment: (A) = 16-22; (B,C) = 3-9. Data are expressed as mean ± SEM . *$p<0.05$.

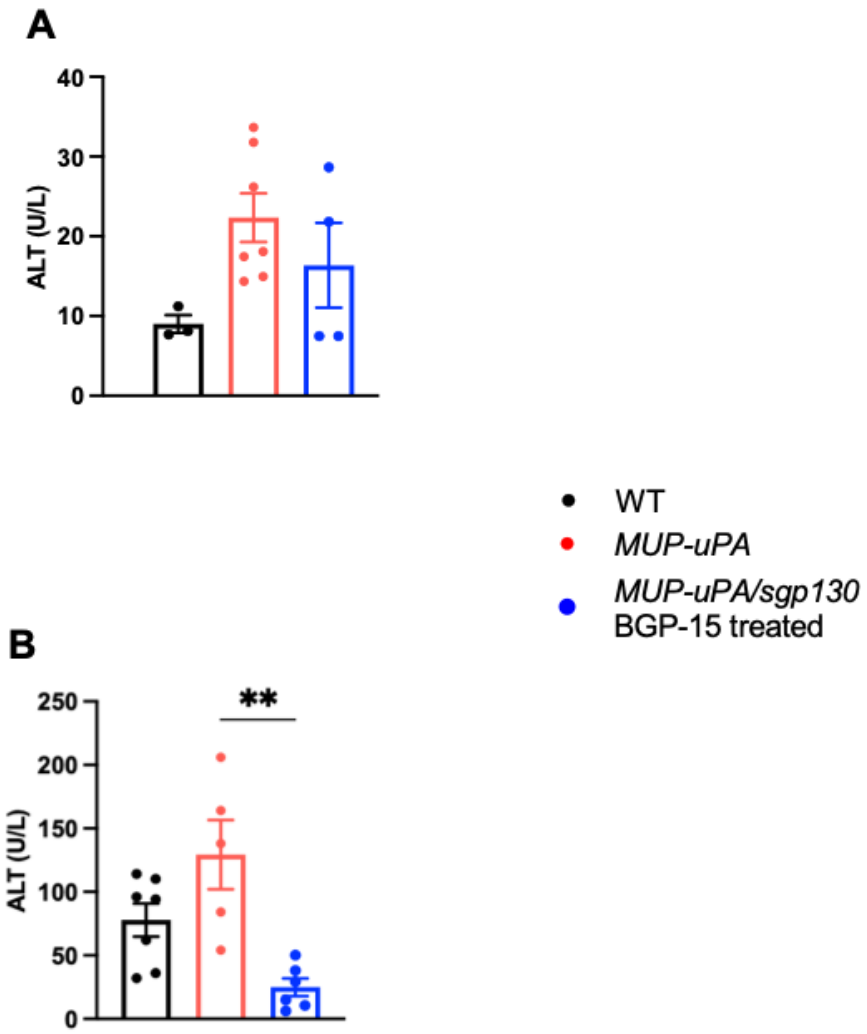

Supplementary Figure 6. Treatment of *MUP-uPA/sgp130Fc* mice with BGP-15 affects liver injury. Plasma alanine aminotransferase (ALT) in blood at 24 wk (A) and 40 wk (B). Data were analysed by one-way ANOVA with Sidak's multiple comparisons. Three to seven biological replicates were used (independent mice) per group. Data are expressed as mean ±SEM. ****p<0.001*.

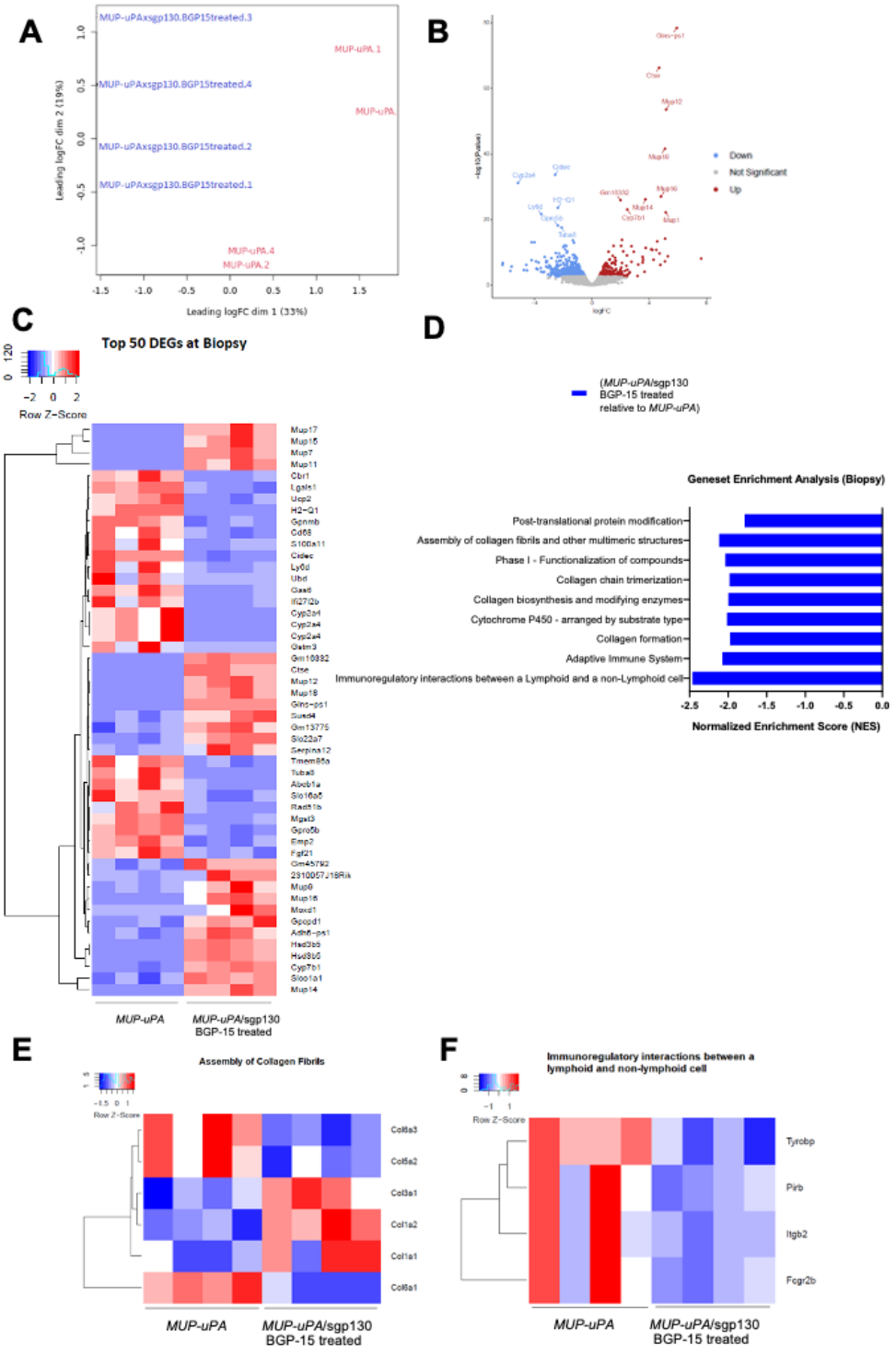

Supplementary Figure 7. RNAseq analyses on liver samples obtained at 24 wk demonstrates that genes controlling collagen formation and immune function are downregulated in MUP-uPA/sgp130 mice treated with BGP-15. Principle component analysis (A) and volcano plots (B). The top ranked differentially expressed genes (C) and pathways, as measured by gene set enrichment analyses (GSEA) (D). Genes controlling collagen deposition (E) and immunoregulatory interactions (F) were among the top gene sets downregulated by sgp130/BGP15 treatment. Four biological replicates (independent mice) were analyzed from each group (n=4). The false discovery rate (FDR) <0.05.

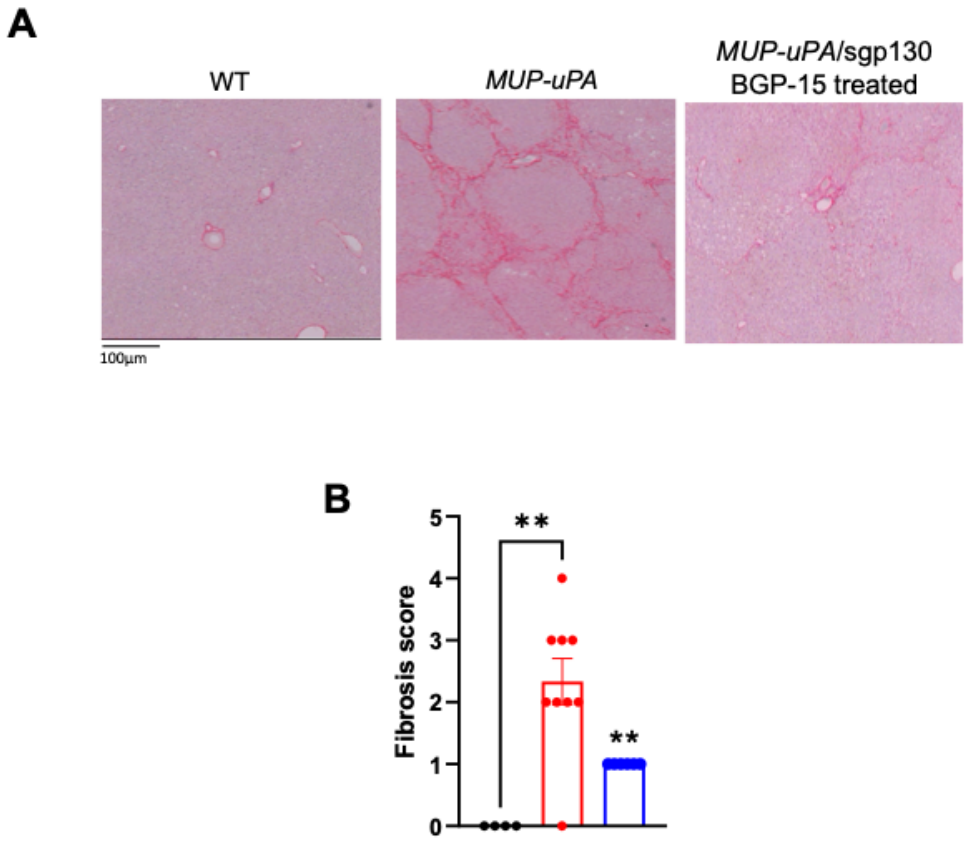

Supplementary Figure 8. Treatment of *MUP-uPA/sgp130Fc* mice with BGP-15 ameliorates markers of NASH at 40 weeks. Representative image (A) and quantification of collagen deposition as an indication of fibrosis (BD) in WT, *MUP-uPA* and *MUP-uPA*/sgp130 BGP-15 treated mice measured by Picosirus Red Staining (PSR). Data were analysed by one-way ANOVA with Sidak's multiple comparisons. The following numbers of biological replicates were used (independent mice) per group in each experiment: (B) = = 4-9. Data are expressed as mean ±SEM .***p<0.01*, ****p<0.001*.

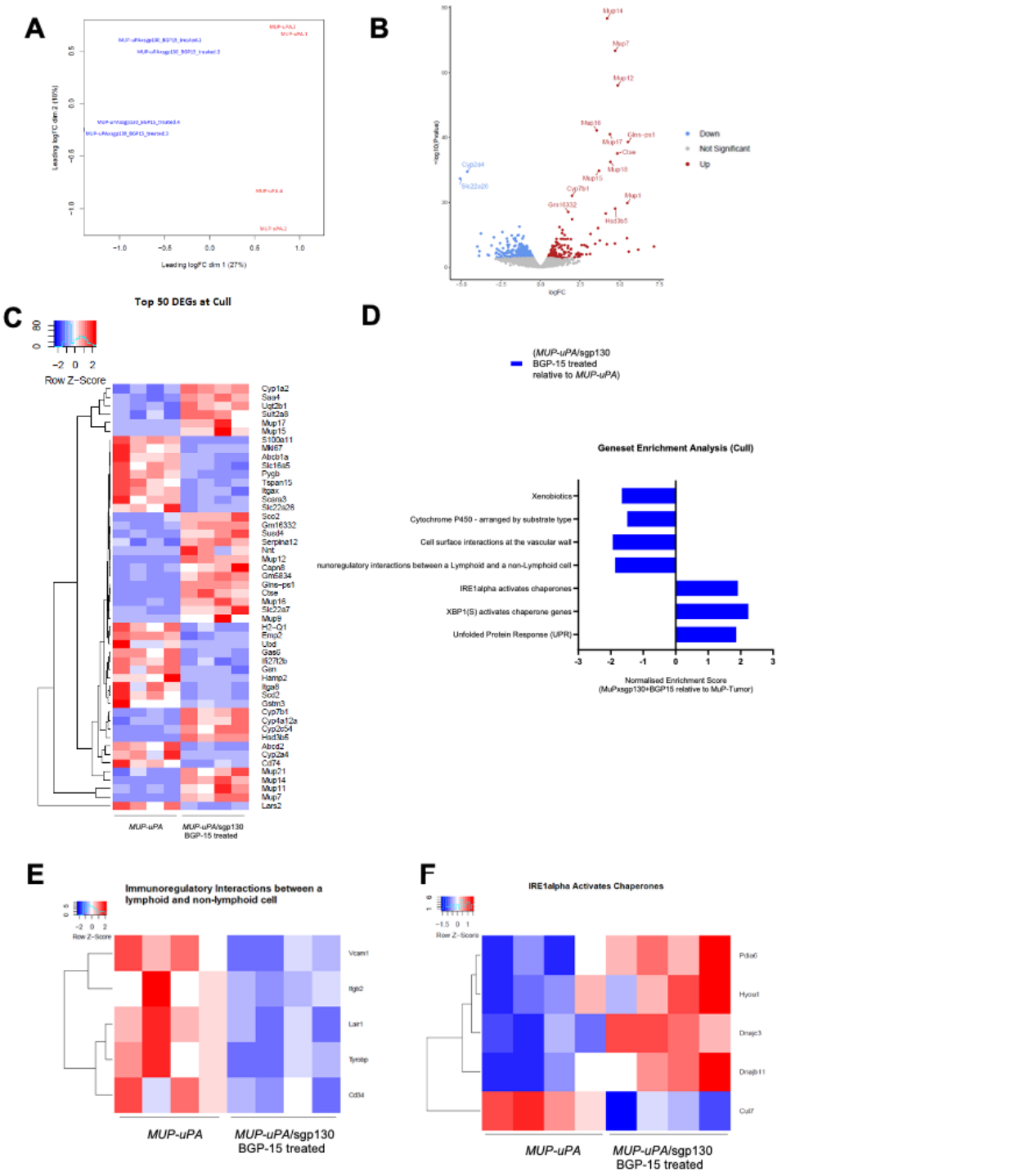

Supplementary Figure 9. RNAseq analyses on liver samples obtained at 40 wk demonstrates that genes controlling immune function are downregulated but genes controlling molecular chaperone pathways are upregulated in MUP-uPA/sgp130 mice treated with BGP-15. Liver samples were obtained at 40 wk. Principle component analysis (A) and volcano plots (B). The top ranked differentially expressed genes (C) and pathways, as measured by gene set enrichment analyses (GSEA) (D). Genes controlling and immunoregulatory interactions (E) and IRE1a (F) were among the top gene sets downregulated or upregulated by sgp130/BGP15 treatment. Four biological replicates (independent mice) were analyzed from each group. The false discovery rate (FDR) <0.05.

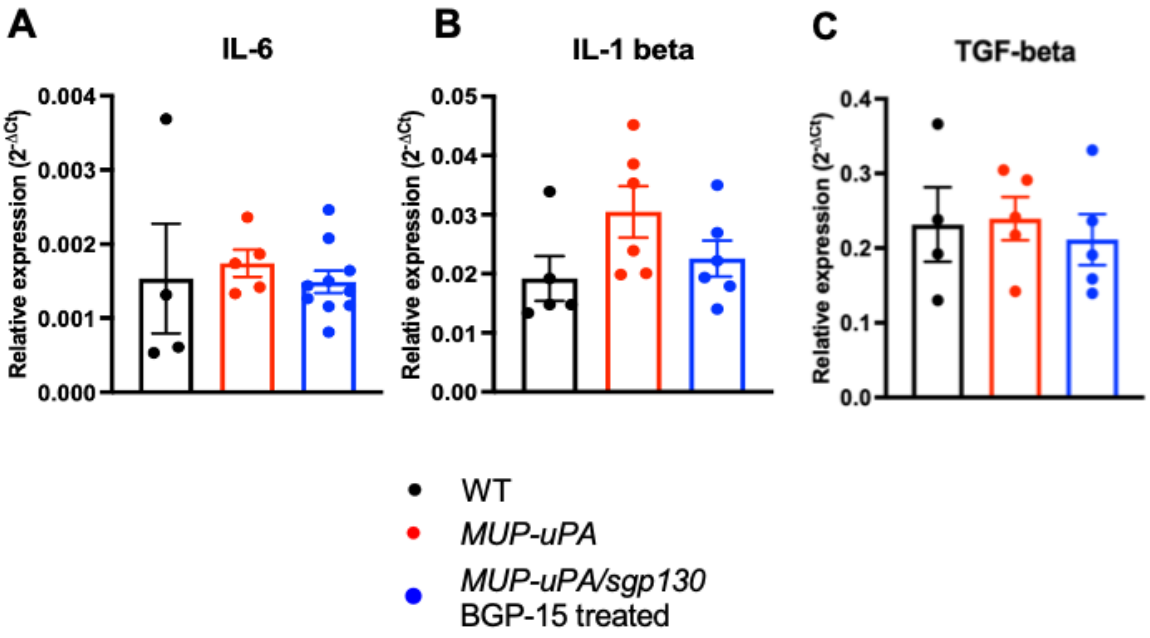

Supplementary Figure 10. Effect of treatment of *MUP-uPA/sgp130Fc* mice with BGP-15 on mRNA transcript level of pro-inflammatory cytokines at 40 weeks. mRNA expression of interleukin-1 beta (IL-1β), interleukin-6 (IL-6) and transforming growth factor beta (TGFβ) in liver samples taken from mice at 40 wk. Data were analyzed by one-way ANOVA with Sidak's multiple comparisons. 4-10 mice were used per group. Data are expressed as mean ±SEM .

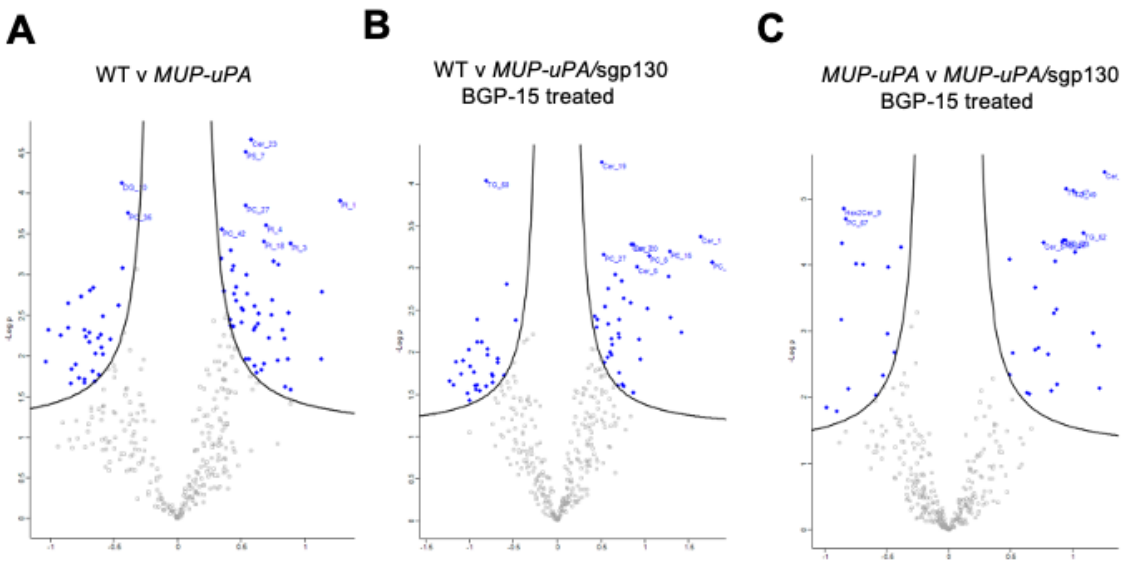

Supplementary Figure 11. *MUP-uPA*/sgp130 mice treated with BGP-15 do not show reduced liver lipids. Liver samples were obtained at 40 wk. Volcano plots showing lipidomic profile of wilt type (WT) mice *MUP-uPA* mice and *MUP-uPA*/sgp130 BGP-15 treated mice. Blue dots indicate individual lipid species that were increased or decreased by comparison. Ten to 18 biological replicates were used (independent mice) per group in each experiment.

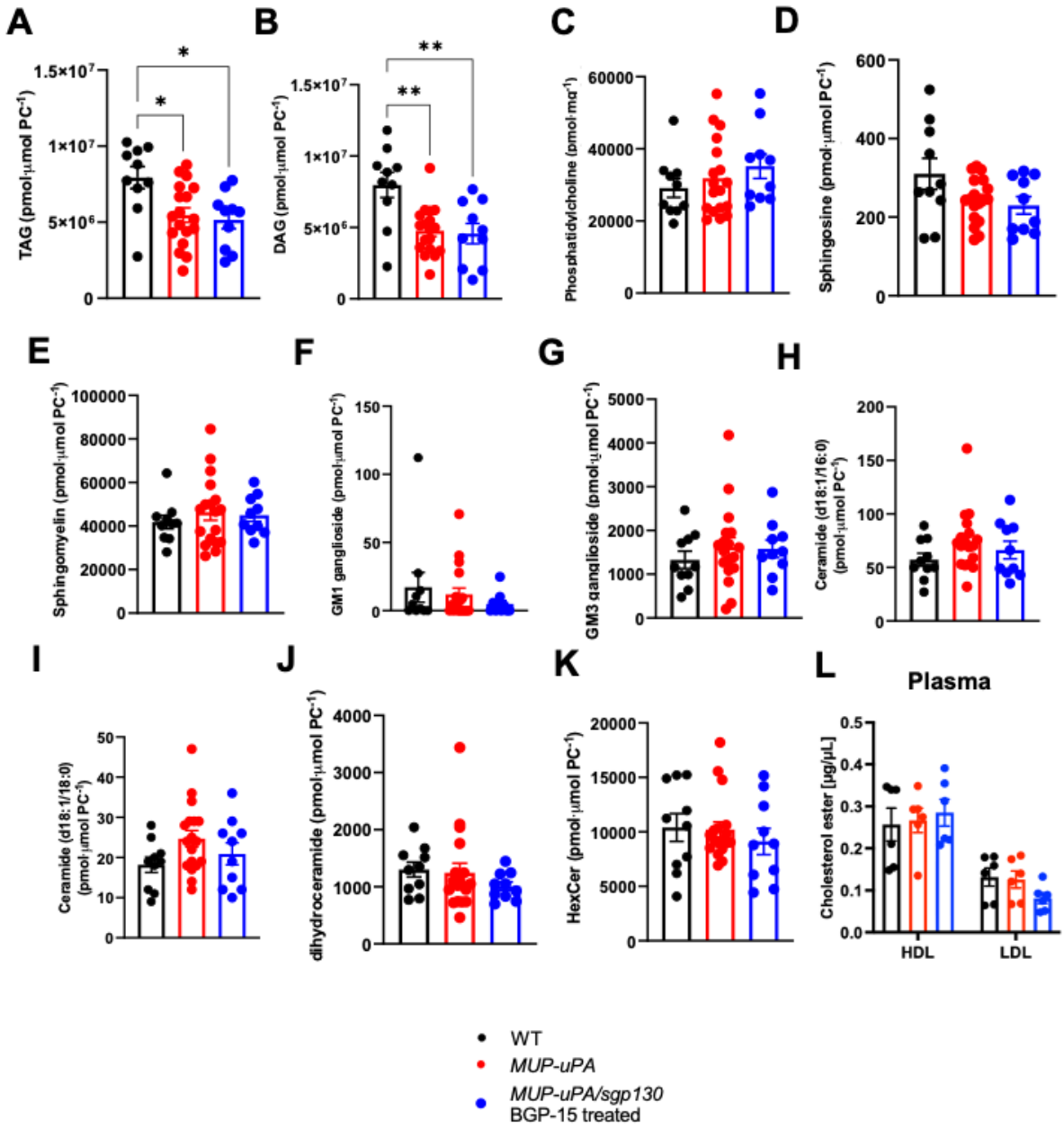

Supplementary Figure 12. *MUP-uPA*/sgp130 mice treated with BGP-15 do not show reduced lipids. Liver samples and blood samples were obtained at 40 wk. Triaclyglycerol (TAG) (A), Diacylglycerol (DAG) (B), Phosphatidylcholine (C), Sphingosine (D), Sphingomyelin (E), GM1 ganglioside (F), GM3 ganglioside (G), Ceramide (d18:1/C16) (H) ceramide (d18:1/C18) (I) Dihydroceramide (J), Hexosylceramide (HexCer) (K), in wild type (WT) mice, *MUP-uPA* mice and *MUP-uPA*/sgp130 mice treated with BGP-15. One-way ANOVA with Tukey's multiple comparisons where indicated. 10-18 biological replicates were used (independent mice) per group in each experiment. Data are expressed as mean ±SEM. *$p<0.05$, **$p<0.01$.

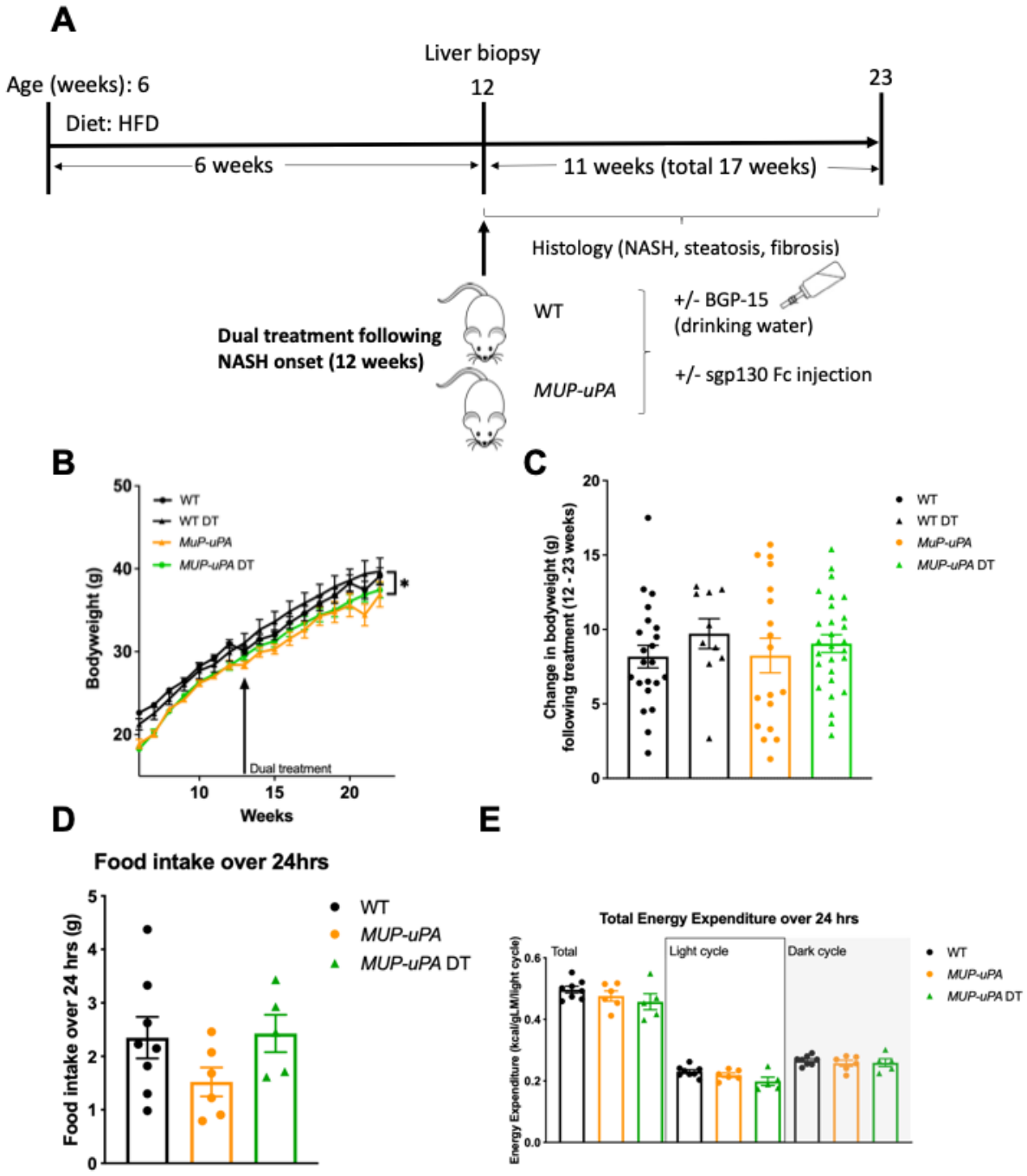

Supplementary Figure 13. Treatment with BGP-15 and sgp130Fc after NASH does not affect body weight gain, food intake or energy expenditure. Wild type (WT) and *MUP-uPA* mice were untreated or treated with BGP-15 (in drinking water and sgp130Fc (twice weekly injections of 0.5 mg/kg)v for 11 wk [double treatment (DT)]. Experimental design (A). Body mass (B) and change in body mass (C), food intake (D) and energy expenditure (E). Data were analysed by one-way ANOVA with Tukey's multiple comparisons. The following numbers of biological replicates were used (independent mice) per group in each experiment: (B-C) = 10-29; (D-E) = 5-8. Data are expressed as mean ±SEM. ***p<0.01*

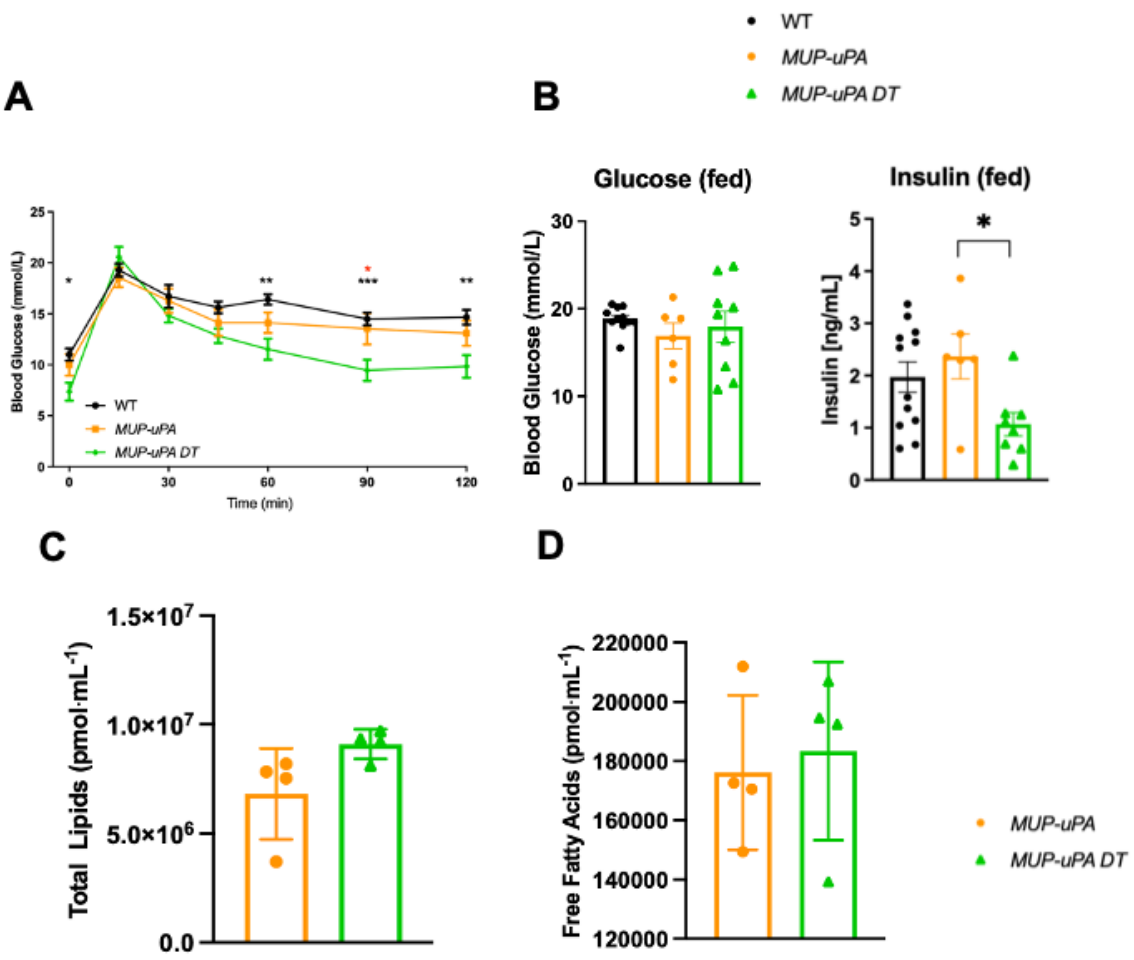

Supplementary Figure 14. Treatment with BGP-15 and sgp130Fc after NASH onset results improved glucose homeostasis but not change in blood lipids. Wild type (WT) and *MUP-uPA* mice were untreated or treated with BGP-15 (in drinking water and sgp130Fc (twice weekly injections of 0.5 mg/kg) for 11 wk [double treatment (DT)]. Blood glucose during an oral glucose tolerance test (A), glucose and insulin (B) after feeding. Total plasma lipids (C) and free fatty acids (D). Data were analysed by 2-way ANOVA with Tukey's multiple comparisons at each time point for (A), one-way ANOVA with Tukey's multiple comparisons (B) and Unpaired t-tests (C,D). The following numbers of biological replicates were used (independent mice) per group in each experiment: (A) = 5-8; (B) = 6-12; (C-D) = 4 .Data are expressed as mean ±SEM. *$p<0.01$, **$p<0.01$, ***$p<0.001$

Supplementary Table Titles

Table S1. List of DEGs across major liver cell types.

Table S2. List of DEGs across myeloid subsets.

Table S3. List of DEGs across hepatocyte subsets.

Table S4. Pseudobulk analysis of all cell types between tumor bearing vs tumor free mice at 24 weeks biopsy.

Table S5. UPR response genes from S. Reich, et al., 2020, and corresponding mouse orthologues.

Table S6. List of DEGs in daHep compared to combined normal hepatocyte clusters.